

# TASK SPECIFIC PRETRAINING WITH NOISY LABELS FOR REMOTE SENSING IMAGE SEGMENTATION

Chenyang Liu<sup>1,2,3</sup>, Conrad M Albrecht<sup>2</sup>, Yi Wang<sup>1</sup>, Xiao Xiang Zhu<sup>1,3</sup>

<sup>1</sup>Data Science in Earth Observation, Technical University of Munich, Germany

<sup>2</sup>Remote Sensing Technology Institute, German Aerospace Center, Germany

<sup>3</sup>Munich Center for Machine Learning (MCML), Germany

## ABSTRACT

Compared to supervised deep learning, self-supervision provides remote sensing a tool to reduce the amount of exact, human-crafted geospatial annotations. While image-level information for unsupervised pretraining efficiently works for various classification downstream tasks, the performance on pixel-level semantic segmentation lags behind in terms of model accuracy. On the contrary, many easily available label sources (e.g., automatic labeling tools and land cover land use products) exist, which can provide a large amount of noisy labels for segmentation model training. In this work, we propose to exploit noisy semantic segmentation maps for model pretraining. Our experiments provide insights on robustness per network layer. The transfer learning settings test the cases when the pretrained encoders are fine-tuned for different label classes and decoders. The results from two datasets indicate the effectiveness of task-specific supervised pretraining with noisy labels. Our findings pave new avenues to improved model accuracy and novel pretraining strategies for efficient remote sensing image segmentation.

**Index Terms**— segmentation, pretraining, noisy labels, encoder, transfer learning

## 1. INTRODUCTION

Deep learning turned into a powerful tool for data mining on vast amounts of remote sensing (RS) imagery [1]. However, efficient training of deep learning models requires a large amount of accurate annotations, which is hard to obtain due

to human labor intensive labeling process. Recently, self-supervised learning (SSL) has demonstrated great success in alleviating this problem by distillation of representative features from unlabeled data [2]. Existing SSL methods such as contrastive learning [3, 4] primarily rely on image-level information. Those turn out suboptimal for semantic segmentation downstream tasks relative to classification tasks [5]. This discrepancy requests alternative strategies to enhance the efficacy of pretrained models for segmentation tasks.

Recent studies indicate that deep learning models may be robust against label noise [6, 7]. Models trained on billions of Instagram image–hashtag pairs without manual dataset curation exhibit excellent transfer learning performance for image classification tasks [8]. Similar results were obtained when pretraining video models on large volumes of noisy social-media video data [9]. In remote sensing, systematic studies have been carried out to employ crowd-sourced maps like OpenStreetMap (OSM) providing large-scale, publicly available labels for pretraining building and road extraction models [10, 11, 12]. Results indicate that OSM labels, though noisy, can significantly reduce human supervision required to successfully train segmentation models in these tasks. Building upon the success of the existing works, we aim to further explore the potential of noisy labels in model pretraining for RS image segmentation tasks. We target to address the following questions:

1. Can supervised pretraining with noisy labels enhance the performance of encoders in general segmentation tasks compared to SSL methods? If so, what is the mechanism behind it?
2. To what extent does the inconsistency of category definitions between pretraining and fine-tuning tasks impact the overall efficacy of the pretrained encoders?
3. Are the encoders pretrained within a given framework useful when transferred to a different framework utilizing separate decoders for downstream tasks?

To answer these questions, we pretrain ResNet encoders in a supervised fashion on noisy labels to compare them with their SSL counterparts pretrained by DINO [3] and MoCo [4]. We assemble two datasets to evaluate model effectiveness:

---

The work is to appear as a conference paper at IEEE IGARSS 2024. The work of C. Liu, C. M. Albrecht, and Y. Wang is funded by the Helmholtz Association through the Framework of *HelmholtzAI*, grant ID: ZT-I-PF-5-01 – *Local Unit Munich Unit @Aeronautics, Space and Transport (MASTr)*. The compute related to this work was supported by the Helmholtz Association’s Initiative and Networking Fund on the HAICORE@FZJ partition. The work of X. X. Zhu is supported by the German Federal Ministry of Education and Research (BMBF) in the framework of the international future AI lab “AI4EO – Artificial Intelligence for Earth Observation: Reasoning, Uncertainties, Ethics and Beyond” (grant number: 01DD20001).

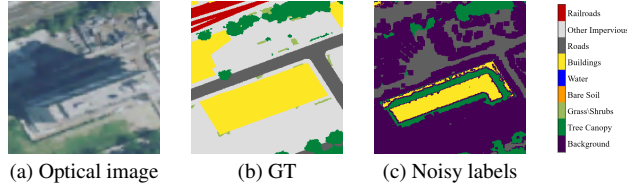


**Fig. 1.** Visualization of a data triple within the NYC dataset.

**Table 1.** Quality assessment of the NYC noisy labels.

CLASS	background	trees	buildings	roads	MEAN
OA					67.83
precision	62.77	78.80	79.76	60.04	70.34
recall	78.72	62.44	60.31	56.89	64.59
IoU	53.67	53.46	52.30	41.26	50.17

- the New York City (NYC) dataset representing a small-scale, in-domain scenario, and
- the SSL4EO-S2DW dataset potentially used for RS foundation model construction.

In the following, we first present the details of the two datasets and our experimental setups in Section 2, followed by results and corresponding discussions in Section 3. We summarize our findings for future lines in Section 4.

## 2. PRETRAINING WITH NOISY LABELS

### 2.1. Datasets

#### 2.1.1. NYC dataset

The New York City (NYC) dataset was collected over New York City in 2017. We picked the 1m spatial resolution orthophotos as inputs. The four spectral bands are: near-infrared (NIR), red (R), green (G), and blue (B). We paired the pixel-level ground truth (GT) masks with 8 categories as depicted to the right of Fig. 1. The noisy labels were generated from LiDAR data using the AutoGeoLabel approach as proposed in [13], yet containing three classes, only: trees, buildings, and roads. Unclassified pixels are annotated as background. All data were curated into small patches of  $288 \times 288$  pixels, cf. Fig. 1. A total of 26,500 data triples (orthophoto, GT, noisy labels) have been curated, with 4,500 hold out for testing. Table 1 quantifies the quality of the noisy labels. We provide this dataset as test for the effectiveness of noisy label pretraining in a small-scale in-domain scenario. 22,000– $X$  data pairs serve pretraining either with or without noisy labels. The fine-tuning is implemented with 100 randomly selected image-GT pairs from the 22,000 pretraining patches.

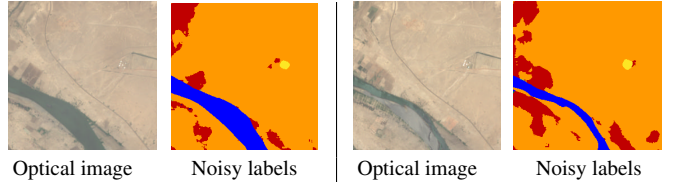


**Fig. 2.** Visualization of orthophotos and corresponding noisy label masks for two seasons (left/right) at a random location of the SSL4EO-S2DW dataset. Blue, red, yellow, and orange represent water, crops, built area, and bare land, respectively.

#### 2.1.2. SSL4EO-S2DW dataset

The dataset termed SSL4EO-S2DW we extend from the SSL4EO-S12 dataset [5], a large-scale self-supervision dataset for Earth observation. SSL4EO-S12 samples data globally from 251,079 locations. Each location corresponds to 4 Sentinel-1 and -2 image pairs of  $264 \times 264$  pixels from each season. Here, we only include Sentinel-2 data for SSL pre-training. We pair them with the 9-class labels from the Google Dynamic World (DW) project [14], cf. Fig. 2. The 9 classes include: water, trees, grass, flooded vegetation, crops, shrub and scrub, built area, bare land, and ice & snow. We curated 103,793 locations with noisy label masks matching all seasons. SSL4EO-S2DW resembles use cases where noisy labels are still a bit harder to obtain than abundant RS imagery. To evaluate pretrained encoders, we utilize the same downstream segmentation tasks as in [5], namely: DFC2020 [15] for land cover classification and OSCD for urban area change detection [16]. We employ the training and test sets of the OSCD dataset. For the DFC2020 dataset, we utilize the 986 validation patches for fine-tuning, and 5128 test images for testing.

### 2.2. Implementation Details

For pretraining, we use image data and noisy label pairs to train U-Nets with ResNet encoder backbones in a standard supervised setup. Given the dataset sizes, we chose ResNet18 (NYC) and ResNet50 (SSL4EO-S2DW). For transfer learning, we test the pretrained encoders within different frameworks: U-Net [17], DeepLabv3++ [18], and PSPNet [19]. Our pretrained encoders are compared with random initialization and those obtained by DINO and MoCo from [5].

We applied an Adam optimizer on a loss combining CrossEntropy and Dice. Random flipping served as our data augmentation strategy. The pretraining learning rate we set to  $1e-3$ . We use a smaller learning rate of  $5e-4$  adjusted by a cos-scheduler for fine-tuning. For SSL4EO-S2DW pre-training, we randomly cropped patches into  $256 \times 256$ , and chose the data from an arbitrary season at each geospatial location and training iteration to act as an additional augmentation strategy. We pretrain the models with a batch size of 256 per GPU. Pre-training for 100 epochs takes about 5

**Table 2.** Fine-tuning results (IoU, %) obtained on the NYC dataset with different frameworks.

Framework	Pretraining	trees	grass/schrubs	bareland	water	buildings	roads	other impervious	railroads	mIoU
U-Net (fixed encoder)	random	46.75	22.78	<b>91.09</b>	<b>96.55</b>	44.69	32.73	30.67	90.86	54.28
	DINO	49.34	22.90	79.38	90.04	46.15	42.31	31.70	91.14	57.09
	MoCo	47.56	22.65	78.76	72.13	47.21	42.27	31.50	91.10	56.52
	noisy labels	<b>58.74</b>	<b>26.97</b>	91.05	81.74	<b>59.37</b>	<b>57.10</b>	<b>39.56</b>	<b>91.20</b>	<b>63.08</b>
DeepLabv3++ (fine-tuned encoder)	random	48.39	19.03	79.11	86.24	48.53	43.20	29.02	<b>90.26</b>	55.28
	DINO	49.61	19.83	72.68	86.44	51.73	44.11	29.20	75.02	53.46
	MoCo	49.13	20.65	69.05	87.41	51.98	47.82	30.24	82.68	54.76
	noisy labels	<b>54.78</b>	<b>23.86</b>	<b>84.41</b>	<b>92.08</b>	<b>59.22</b>	<b>58.04</b>	<b>37.99</b>	81.10	<b>61.31</b>

**Table 3.** Fine-tuning results (%) obtained on the DFC2020 dataset using PSPNet as frameworks, where OA presents overall accuracy, and AA is average accuracy.

Pretraining	fixed encoder			fine-tuned encoder		
	OA	mIoU	AA	OA	mIoU	AA
random	56.42	31.50	45.12	58.68	33.56	46.03
DINO	64.82	37.81	48.83	63.64	36.95	49.92
MoCo	63.25	37.67	51.00	61.19	34.86	47.29
noisy labels	<b>66.66</b>	<b>40.88</b>	<b>53.24</b>	<b>67.11</b>	<b>41.06</b>	<b>53.14</b>

hours on an NVIDIA A100 GPU with the NYC dataset. For SSL4EO-S2DW it takes 4 GPUs to train for 100 epochs in 6 hours.

### 3. EXPERIMENTAL RESULTS

#### 3.1. Transfer Learning

##### 3.1.1. NYC dataset

We transfer the (3+1)-class noisy label pretrained encoder to an 8-class land cover land use segmentation downstream task. While we freeze the encoder when the downstream task utilizes the same framework as in pretraining (U-Net), we let adjust the encoder weights along with the decoder when adopting a different framework (DeepLabv3++). As shown in Table 2, the noisy label pretrained encoder outperforms the other models on almost all classes although the pretrained model has not been pretrained on some of the classes: Including semantic information for pretraining is beneficial for models to learn generic features that are discriminative for semantic segmentation downstream tasks. Notably, the pretrained encoder works for different training frameworks, too. In this case, pretrained encoders seem compatible when transferred to, e.g., DeepLabv3++. In contrast, the two SSL methods fail to show an edge over random initialization on the NYC dataset. We partly attribute this result to a lack of large amounts of unlabeled data in a small-scale setup.

##### 3.1.2. SSL4EO-S2DW dataset

We picked PSPNet and U-Net as frameworks for the DFC2020 and OSCD datasets. We test two fine-tuning settings with

**Table 4.** Fine-tuning results (%) obtained on the OSCD dataset using U-Net as frameworks.

Pretraining	fixed encoder			fine-tuned encoder		
	OA	IoU	Precision	OA	IoU	Precision
random	95.47	17.08	<b>78.06</b>	95.16	21.80	66.27
DINO	95.59	21.74	73.83	95.53	31.05	66.45
MoCo	95.66	23.81	73.34	95.70	32.56	66.39
noisy labels	<b>95.79</b>	<b>26.80</b>	73.90	<b>95.98</b>	<b>33.37</b>	<b>71.34</b>

fixed and fine-tuned encoders on both datasets. Table 3 and Table 4 present results, respectively. Noisy label-pretrained encoders yield better results when compared to SSL-pretraining or when referenced to random initialization. Performance margins increase when the encoders are fixed in the fine-tuning stage, which indicates that the encoder pretrained with noisy labels is able to generate features adapted to segmentation tasks. Our experiments on two distinct downstream tasks further illustrate the generalizability of encoders pretrained by noisy labels.

#### 3.2. Impact of Label Noise on Model Training

To understand the mechanism behind the success of noisy label pretraining, we utilize a 3-class version of the NYC dataset discriminating trees, buildings, and background as illustrated in Fig. 3. We train two U-Net models from scratch employing all available training patches; one with noisy labels and one with exact labels (GT masks), respectively. After training, we analyze the output features of each convolutional layer of the U-Net given an input patch. For one input patch, we visualize the first principle component of each such output feature data cube in Fig. 3. We observe:

- the encoder features visually share spatial characteristics, i.e., the encoder seems little impacted by label noise
- the closer the convolutional layer gets to the U-Net’s output, the more the features become contaminated by label noise

Since the encoder learns to extract basic spatial features from local semantic information of the input data, it is affected little by label noise. In terms of backpropagation, decoders are

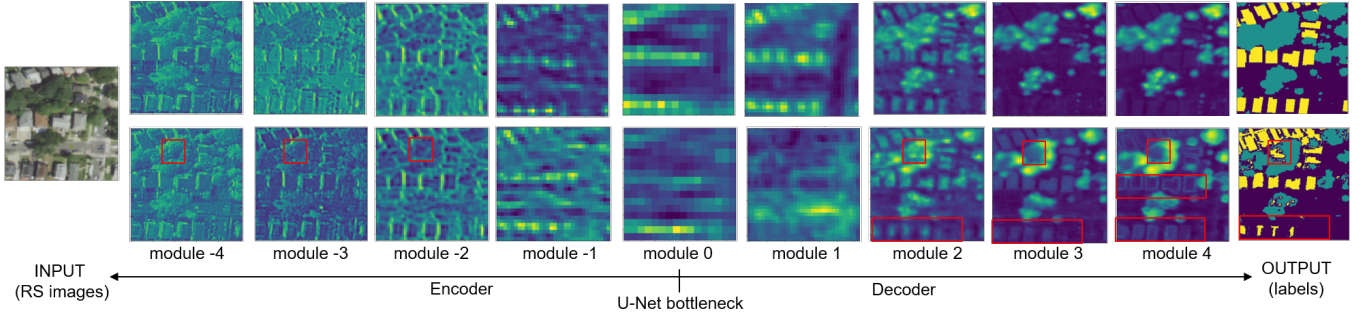


**Fig. 3.** Visualization of the dominant principle component from the output of each convolutional layer of the U-Net model trained with exact labels (top row) and noisy labels (bottom row).

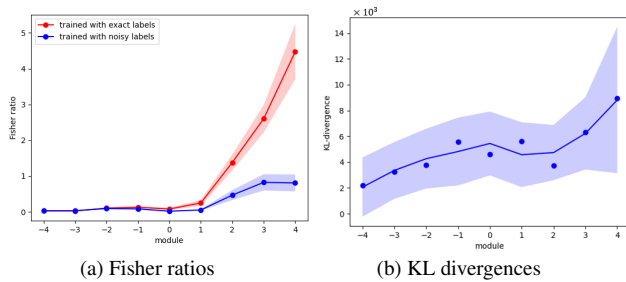


**Fig. 4.** Quantitative assessment of data statistics for convolutional modules after U-Net training: (a) Fisher ratios of module output features after U-Net training. Shaded areas indicate standard deviations w.r.t. data samples investigated. (b) KL divergence of module weight statistics comparing the model trained with exact labels to the one trained on noisy labels. The solid line connects the smoothed results by a Savitzky–Golay filter, and the shaded areas indicates the standard deviation independently training 5 models from scratch.

closer to the (noisy) label mask to optimize the U-Net’s output on. Thus, while the decoder adapts to output noisy labels, the encoder is less biased by label noise.

To quantify our observations, we calculate the Fisher ratios of output feature cubes as presented in Fig. 4 (a). The Fisher ratio is a widely used index to assess feature discrimination in pattern recognition [20]: Larger values indicate better discrimination of features. Two insights we read from Fig. 4:

1. decoder features, whether trained on noisy or exact labels, are more discriminative compared to encoder features
2. the discriminative character of decoder features is degraded when the model is trained on noisy labels, i.e., the decoder is significantly affected by label noise

We did also investigate the model training with exact and noisy labels by computing the Kullback–Leibler (KL) divergence [21] of weight statistics within each module. As demonstrated in Fig. 4 (b), the convolutional layers in the

encoder are governed by similar weight statistics, while those in the decoder follow diverging weight statistics towards the semantic segmentation outputs. Those observations highlight that encoder features are less biased by label noise, yet, they benefit from the semantics provided by pixel-level noisy label masks.

#### 4. CONCLUSIONS & PERSPECTIVES

In this work, we explored the effectiveness of pixel-wise noisy labels for pre-training deep artificial neural networks on semantic segmentation downstream tasks. Experiments utilizing two remote sensing datasets demonstrate the potential of the proposed approach in order to enhance the performance of encoder networks for various segmentation downstream tasks—even when the class definitions or the training frameworks of fine-tuning divert from the pretraining setup. Furthermore, we tapped on explaining why encoders seem robust against label noise for U-Net models. Our findings motivate future work to test the pretrained encoders on a more diverse set of downstream tasks. Additional experiments beyond U-Net training will help to solidify our initial observations.

#### 5. REFERENCES

- [1] Xiao Xiang Zhu, Devis Tuia, Lichao Mou, Gui-Song Xia, Liangpei Zhang, Feng Xu, and Friedrich Fraundorfer, “Deep learning in remote sensing: A comprehensive review and list of resources,” *IEEE geoscience and remote sensing magazine*, vol. 5, no. 4, pp. 8–36, 2017, Publisher: IEEE.
- [2] Yi Wang, Conrad M. Albrecht, Nassim Ait Ali Braham, Lichao Mou, and Xiao Xiang Zhu, “Self-Supervised Learning in Remote Sensing: A review,” *IEEE Geoscience and Remote Sensing Magazine*, vol. 10, no. 4, pp. 213–247, Dec. 2022, Conference Name: IEEE Geoscience and Remote Sensing Magazine.

- [3] Mathilde Caron, Hugo Touvron, Ishan Misra, Hervé Jégou, Julien Mairal, Piotr Bojanowski, and Armand Joulin, “Emerging Properties in Self-Supervised Vision Transformers,” 2021, pp. 9650–9660.
- [4] Kaiming He, Haoqi Fan, Yuxin Wu, Saining Xie, and Ross Girshick, “Momentum Contrast for Unsupervised Visual Representation Learning,” 2020, pp. 9729–9738.
- [5] Yi Wang, Nassim Ait Ali Braham, Zhitong Xiong, Chenying Liu, Conrad M. Albrecht, and Xiao Xiang Zhu, “SSL4EO-S12: A large-scale multimodal, multitemporal dataset for self-supervised learning in Earth observation [Software and Data Sets],” *IEEE Geoscience and Remote Sensing Magazine*, vol. 11, no. 3, pp. 98–106, Sept. 2023.
- [6] Chiyuan Zhang, Samy Bengio, Moritz Hardt, Benjamin Recht, and Oriol Vinyals, “Understanding deep learning (still) requires rethinking generalization,” *Communications of the ACM*, vol. 64, no. 3, pp. 107–115, Feb. 2021, Number: 3.
- [7] Chenying Liu, Conrad M Albrecht, Yi Wang, and Xiao Xiang Zhu, “Peaks Fusion assisted Early-stopping Strategy for Overhead Imagery Segmentation with Noisy Labels,” in *2022 IEEE International Conference on Big Data (Big Data)*, Dec. 2022, pp. 4842–4847.
- [8] Dhruv Mahajan, Ross Girshick, Vignesh Ramanathan, Kaiming He, Manohar Paluri, Yixuan Li, Ashwin Bharambe, and Laurens van der Maaten, “Exploring the Limits of Weakly Supervised Pretraining,” 2018, pp. 181–196.
- [9] Deepti Ghadiyaram, Du Tran, and Dhruv Mahajan, “Large-Scale Weakly-Supervised Pre-Training for Video Action Recognition,” 2019, pp. 12046–12055.
- [10] Pascal Kaiser, Jan Dirk Wegner, Aurélien Lucchi, Martin Jaggi, Thomas Hofmann, and Konrad Schindler, “Learning Aerial Image Segmentation From Online Maps,” *IEEE Transactions on Geoscience and Remote Sensing*, vol. 55, no. 11, pp. 6054–6068, Nov. 2017, Number: 11.
- [11] Emmanuel Maggiori, Yuliya Tarabalka, Guillaume Charpiat, and Pierre Alliez, “Convolutional Neural Networks for Large-Scale Remote-Sensing Image Classification,” *IEEE Transactions on Geoscience and Remote Sensing*, vol. 55, no. 2, pp. 645–657, Feb. 2017, Number: 2.
- [12] Rui Zhang, Conrad Albrecht, Wei Zhang, Xiaodong Cui, Ulrich Finkler, David Kung, and Siyuan Lu, “Map generation from large scale incomplete and inaccurate data labels,” in *Proceedings of the 26th ACM SIGKDD International Conference on Knowledge Discovery & Data Mining*, 2020, pp. 2514–2522.
- [13] Conrad M Albrecht, Fernando Marianno, and Levente J Klein, “AutoGeoLabel: Automated Label Generation for Geospatial Machine Learning,” in *2021 IEEE International Conference on Big Data (Big Data)*, Dec. 2021, pp. 1779–1786.
- [14] Christopher F. Brown, Steven P. Brumby, Brookie Guzder-Williams, Tanya Birch, Samantha Brooks Hyde, Joseph Mazzariello, Wanda Czerwinski, Valerie J. Pasquarella, Robert Haertel, Simon Ilyushchenko, Kurt Schwehr, Mikaela Weisse, Fred Stolle, Craig Hanson, Oliver Guinan, Rebecca Moore, and Alexander M. Tait, “Dynamic World, Near real-time global 10 m land use land cover mapping,” *Scientific Data*, vol. 9, no. 1, pp. 251, June 2022, Number: 1.
- [15] Naoto Yokoya, “2020 IEEE GRSS Data Fusion Contest,” Dec. 2019.
- [16] Rodrigo Caye Daudt, Bertr Le Saux, Alexandre Boulch, and Yann Gousseau, “Urban Change Detection for Multispectral Earth Observation Using Convolutional Neural Networks,” in *IGARSS 2018 - 2018 IEEE International Geoscience and Remote Sensing Symposium*, July 2018, pp. 2115–2118, ISSN: 2153-7003.
- [17] Olaf Ronneberger, Philipp Fischer, and Thomas Brox, “U-Net: Convolutional Networks for Biomedical Image Segmentation,” in *Medical Image Computing and Computer-Assisted Intervention – MICCAI 2015*, Nassir Navab, Joachim Hornegger, William M. Wells, and Alejandro F. Frangi, Eds., Cham, 2015, Lecture Notes in Computer Science, pp. 234–241, Springer International Publishing.
- [18] Liang-Chieh Chen, Yukun Zhu, George Papandreou, Florian Schroff, and Hartwig Adam, “Encoder-Decoder with Atrous Separable Convolution for Semantic Image Segmentation,” in *Proceedings of the European Conference on Computer Vision (ECCV)*, 2018, pp. 801–818.
- [19] Hengshuang Zhao, Jianping Shi, Xiaojuan Qi, Xiaogang Wang, and Jiaya Jia, “Pyramid Scene Parsing Network,” in *Proceedings of the IEEE Conference on Computer Vision and Pattern Recognition*, 2017, pp. 2881–2890.
- [20] Chenying Liu, Lin He, Zhetao Li, and Jun Li, “Feature-Driven Active Learning for Hyperspectral Image Classification,” *IEEE Transactions on Geoscience and Remote Sensing*, vol. 56, no. 1, pp. 341–354, Jan. 2018, Conference Name: IEEE Transactions on Geoscience and Remote Sensing.

- [21] David J. C. MacKay, *Information Theory, Inference and Learning Algorithms*, Cambridge University Press, Sept. 2003, Google-Books-ID: AKuMj4PN.EMC.